Available online at www.sciencedirect.com
ScienceDirect
Journal of Computational and Applied Mathematics 205 (2007) 251–271
JOURNAL OF COMPUTATIONAL AND APPLIED MATHEMATICS
www.elsevier.com/locate/cam

Numerical analysis of free vibrations of laminated composite conical and cylindrical shells: Discrete singular convolution (DSC) approach

Ömer Civalek*

Akdeniz University, Engineering Faculty, Civil Engineering Department, Division of Mechanics, 07200, Topcular, Antalya, Turkiye

Received 11 April 2005; received in revised form 14 March 2006

Abstract

A numerical study on the free vibration analysis for laminated conical and cylindrical shell is presented. The analysis is carried out using Love's first approximation thin shell theory and solved using discrete singular convolution (DSC) method. Numerical results in free vibrations of laminated conical and cylindrical shells are presented graphically for different geometric and material parameters. Free vibrations of isotropic cylindrical shells and annular plates are treated as special cases. The effects of circumferential wave number, number of layers on frequencies characteristics are also discussed. The numerical results show that the present method is quite easy to implement, accurate and efficient for the problems considered.

Keywords: Free vibration; Numerical approach; Discrete singular convolution; Laminated conical shells; Cylindrical shell; Frequencies

1. Introduction

Laminated composite materials are increasingly used in aerospace, mechanical and civil engineering structures. With the increasing use of fiber-reinforced composites as structural elements, studies including the linear and nonlinear vibration of composite material shell are receiving considerable attention. This arises from the fact that, by taking advantage of its anisotropic material properties and light weight with high strength, the materials can be used very efficiently [2,32]. Because of the practical importance of the free vibration analysis of the composite laminated conical shell in structural, aerospace, nuclear, petrochemical, submarine hulls, and mechanical applications, a few investigators have made efforts to deal with free vibration analysis of this type of structures. Various methods for analyzing free vibrations of the conical shell such as the finite element method, Ritz method, Galerkin method, the other numerical approximate methods and the differential quadrature method have been tried. Unsymmetric free vibration of orthotropic sandwich shells of revolution has been made by Bacon and Bert [1]. Siu and Bert [36] analyzed the free vibration of isotropic and orthotropic conical shells by using the Rayleigh–Ritz technique. Irie et al. [10,11] developed a transfer-matrix approach for free vibration of conical shells with constant and variable thickness. Using the finite element method, Sivadas and Ganesan [37] analyzed the free vibration of conical shells with uniform thickness. Yang [55]

* Tel.: +90 242 323 2364; fax: +90 242 323 2362.
E-mail address: civalek@yahoo.com.

0377-0427/$ - see front matter © 2006 Elsevier B.V. All rights reserved.
doi:10.1016/j.cam.2006.05.001

adopted the integration method in the vibration analysis of orthotropic conical shells. Tong [39–41], in a series of papers, examined the vibration and buckling analysis of isotropic, orthotropic and laminated conical shells by the power series expansion method. More recently, Shu [33,34], Shu and Du [35], Hua [7,8], Hua and Lam [9] and Lam and Hua [13] presented the differential quadrature method to study the free vibration of orthotropic and laminated rotating conical shells. Liew et al. [19] also studied the effects of initial twist and thickness variation on the vibration behavior of shallow conical shells. Lim and Kitipornchai [22] proposed the effects of subtended and vertex angles of the free vibration of open conical shell and panels. Vibration characteristics of conical shell panels with three-dimensional flexibility have been given in detail [16]. Some selected works in this research topic includes those of Liew et al. [21,17,20], Liew and Lim [18], Lim and Liew [25–27], Lim et al. [29,28,24], Lam and Loy [14], Wu and Wu [54], Leissa [15], Soedel [38] and Civalek [4–6]. More detailed information can be found in a recent review paper by Chang [3] and Kapania [12].

The focus in this work is on the application of the DSC method to the differential equation, which governs the free vibration analysis of laminated conical and cylindrical shells.

2. Governing equations

Consider a laminated conical shell of thickness h, cone semivertex angle α and cone length L as shown in Fig. 1. R_1 and R_2 are the radii of the cone at its small and large edges. The conical shell is referred to a coordinate system (x, θ, z) as shown in Fig. 1. The components of the deformation of the conical shell with references to this given coordinate system are denoted by u, v, w in the x, θ and z directions, respectively. The equilibrium equation of motion in terms of the force and moment resultants can be written as [40]

$$\frac{\partial N_x}{\partial x} + \frac{1}{R(x)}\frac{\partial N_{x\theta}}{\partial \theta} + \frac{\sin\alpha}{R(x)}(N_x - N_\theta) = \rho h \frac{\partial^2 u}{\partial t^2}, \tag{1}$$

$$\frac{\partial N_{x\theta}}{\partial x} + \frac{1}{R(x)}\frac{\partial N_\theta}{\partial \theta} + \frac{\cos\alpha}{R(x)}\frac{\partial M_{x\theta}}{\partial x} + \frac{\cos^2\alpha}{R^2(x)}\frac{\partial M_\theta}{\partial \theta} + 2\frac{\sin\alpha}{R(x)}N_{x\theta} = \rho h \frac{\partial^2 v}{\partial t^2}, \tag{2}$$

$$\frac{\partial^2 M_x}{\partial x^2} + \frac{2}{R(x)}\frac{\partial^2 M_{x\theta}}{\partial \theta \partial x} + \frac{1}{R^2(x)}\frac{\partial^2 M_\theta}{\partial \theta^2} + \frac{2\sin\alpha}{R(x)}\frac{\partial M_x}{\partial x} - \frac{1}{R(x)}\left(\sin\alpha\frac{\partial M_\theta}{\partial x} + \cos\alpha N_\theta\right) = \rho h \frac{\partial^2 w}{\partial t^2}, \tag{3}$$

where

$$R(x) = R_1 + x\sin\alpha, \tag{4}$$

$$\rho_a(x, \theta) = \frac{1}{h}\int_{-h/2}^{h/2} \rho(x, \theta, z)\,\mathrm{d}z, \tag{5}$$

here ρ and ρ_a are, respectively, the density and density per unit length. Moment resultants and in-surface force can be obtained by

$$N = (N_x, N_\theta, N_{x\theta})^{\mathrm{T}} = \int_{-h/2}^{h/2} (\sigma_x, \sigma_\theta, \sigma_{x\theta})^{\mathrm{T}}\,\mathrm{d}z, \tag{6}$$

$$M = (M_x, M_\theta, M_{x\theta})^{\mathrm{T}} = \int_{-h/2}^{h/2} (\sigma_x, \sigma_\theta, \sigma_{x\theta})^{\mathrm{T}} z\,\mathrm{d}z, \tag{7}$$

where the stress vector field is defined by $(\sigma)^{\mathrm{T}} = \{\sigma_x, \sigma_\theta, \sigma_{x\theta}\}$. The stress vector of the kth layer for laminated composite conical shells in which each layer is orthotropic is

$$\{\sigma_k\} = [Q^*_{ij}]\{\varepsilon^*_k\}, \tag{8}$$

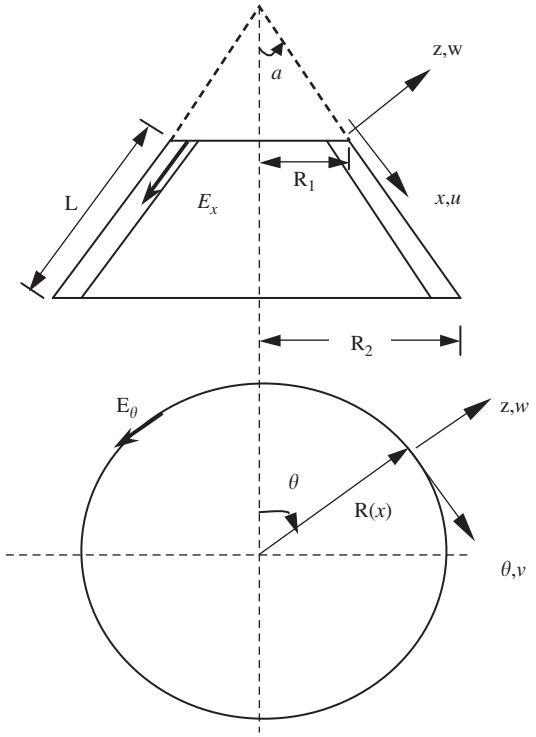

Fig. 1. Geometry and notation of laminated conical shell.

where $\{\varepsilon_k^*\}^{\mathrm{T}}=\{\varepsilon_x, \varepsilon_\theta, \varepsilon_{x\theta}\}$ is the strain vector. Based on the Love's first approximation theory [30], the strain components of this vector are defined as linear functions of the normal (thickness) coordinate z, namely

$$\varepsilon_x = \varepsilon_1 + z\kappa_1, \quad \varepsilon_\theta = \varepsilon_2 + z\kappa_2, \quad \varepsilon_{x\theta} = \gamma + 2z\tau, \tag{9}$$

where $\{\varepsilon\}^{\mathrm{T}} = \{\varepsilon_1, \varepsilon_2, \gamma\}$ and $\{\kappa\}^{\mathrm{T}} = \{\kappa_1, \kappa_2, 2\tau\}$ are, respectively, the strain and curvature vectors of the reference surface. They are defined by

$$\varepsilon_1 = \frac{\partial u}{\partial x}, \quad \varepsilon_2 = \frac{1}{R(x)}\frac{\partial v}{\partial \theta} + \frac{u\sin\alpha}{R(x)} + \frac{w\cos\alpha}{R(x)}, \quad \gamma = \frac{1}{R(x)}\frac{\partial u}{\partial \theta} + \frac{\partial v}{\partial x} - \frac{v\sin\alpha}{R(x)},$$

$$\kappa_1 = -\frac{\partial^2 w}{\partial x^2}, \quad \kappa_2 = -\frac{1}{R^2(x)}\frac{\partial^2 w}{\partial \theta^2} + \frac{\cos\alpha}{R^2(x)}\frac{\partial v}{\partial \theta} - \frac{\sin\alpha}{R(x)}\frac{\partial w}{\partial x},$$

$$\tau = \left[-\frac{1}{R(x)}\frac{\partial^2 w}{\partial x \partial \theta} + \frac{\sin\alpha}{R^2(x)}\frac{\partial w}{\partial \theta} + \frac{\cos\alpha}{R(x)}\frac{\partial v}{\partial x} - \frac{v\sin\alpha\cos\alpha}{R^2(x)}\right]. \tag{10}$$

For a thin and generally orthotropic layer, the stresses defined in Eq. (8) are given by

$$\begin{Bmatrix} \sigma_x \\ \sigma_\theta \\ \sigma_{x\theta} \end{Bmatrix} = \begin{bmatrix} Q_{11}^* & Q_{12}^* & Q_{16}^* \\ Q_{12}^* & Q_{22}^* & Q_{26}^* \\ Q_{16}^* & Q_{26}^* & Q_{66}^* \end{bmatrix} \begin{Bmatrix} \varepsilon_x \\ \varepsilon_\theta \\ \varepsilon_{\theta x} \end{Bmatrix}, \tag{11}$$

where the transformed reduced stiffness matrix of the kth layer is defined by

$$[Q_k^*] = [T][Q_k][T]^{-1}, \tag{12}$$

where

$$[T]=\begin{bmatrix}\cos^2\varphi & \sin^2\varphi & 2\sin\varphi\cos\varphi\\ \sin^2\varphi & \cos^2\varphi & -2\sin\varphi\cos\varphi\\ -\sin\varphi\cos\varphi & \sin\varphi\cos\varphi & \cos^2\varphi-\sin^2\varphi\end{bmatrix} \tag{13}$$

in which $[T]$ is the transformation matrix between the material principal coordinate of the kth layer and the geometric coordinate of the laminated composite conical shell; φ is the angle between these two coordinate directions. The force and moment resultants are given in terms of displacements u, v and w by

$$\begin{Bmatrix}N_x\\ N_\theta\\ N_{x\theta}\\ M_x\\ M_\theta\\ M_{x\theta}\end{Bmatrix}=\begin{bmatrix}c_{11} & c_{12} & c_{13}\\ c_{21} & c_{22} & c_{23}\\ c_{31} & c_{32} & c_{33}\\ c_{41} & c_{42} & c_{43}\\ c_{51} & c_{52} & c_{53}\\ c_{61} & c_{62} & c_{63}\end{bmatrix}\begin{Bmatrix}u\\ v\\ w\end{Bmatrix}, \tag{14}$$

where

$$c_{i1}=A_{i1}\frac{\partial}{\partial x}+A_{i2}\frac{\sin\alpha}{R(x)},$$

$$c_{i2}=\frac{A_{i2}}{R(x)}\frac{\partial}{\partial\theta},$$

$$c_{i3}=-A_{i2}\frac{\cos\alpha}{R(x)}-B_{1i}\frac{\partial^2}{\partial x^2}-B_{i2}\frac{\sin\alpha}{R(x)}\frac{\partial}{\partial x}-\frac{B_{i2}}{R^2(x)}\frac{\partial^2}{\partial\theta^2}$$

$$c_{31}=\frac{A_{66}}{R(x)}\frac{\partial}{\partial\theta},$$

$$c_{32}=A_{66}\left(\frac{\partial}{\partial x}-\frac{\sin\alpha}{R(x)}\right),$$

$$c_{33}=-B_{66}\frac{\partial}{\partial x}\left(\frac{1}{R(x)}\frac{\partial}{\partial\theta}\right),$$

$$c_{ji}=B_{1i}\frac{\partial}{\partial x}+\frac{B_{i2}\sin\alpha}{R(x)},$$

$$c_{j2}=\frac{B_{i2}}{R(x)}\frac{\partial}{\partial\theta},$$

$$c_{j3}=-D_{1i}\frac{\partial^2}{\partial x^2}-D_{i2}\frac{\sin\alpha}{R(x)}\frac{\partial}{\partial x}-\frac{D_{i2}}{R^2(x)}\frac{\partial^2}{\partial\theta^2}-B_{i2}\frac{\cos\alpha}{R(x)},$$

$$c_{61}=\frac{B_{66}}{R(x)}\frac{\partial}{\partial\theta},$$

$$c_{62}=B_{66}\left(\frac{\partial}{\partial x}-\frac{\sin\alpha}{R(x)}\right),$$

$$c_{63}=-2D_{66}\frac{\partial}{\partial x}\left[\frac{1}{R(x)}\frac{\partial}{\partial\theta}\right], \tag{15}$$

where $i = 1, 2$ and $j = 3 + i$. A_{ij}, B_{ij} and D_{ij} are the extensional, coupling and bending stiffnesses and calculated from the following equations:

$$(A_{ij}, B_{ij}, D_{ij}) = \int_{-h/2}^{h/2} Q_{ij}^{*}(1, z, z^2)\,\mathrm{d}z. \tag{16}$$

For an arbitrarily laminated composite shell, these stiffnesses can be given as

$$(A_{ij}) = \sum_{k=1}^{N_L} Q_{ij}^{(k)}(h_k - h_{k-1}), \quad (B_{ij}) = \frac{1}{3}\sum_{k=1}^{N_L} Q_{ij}^{(k)}(h_k^2 - h_{k-1}^2), \quad (D_{ij}) = \frac{1}{3}\sum_{k=1}^{N_L} Q_{ij}^{(k)}(h_k^3 - h_{k-1}^3), \tag{17}$$

where N_L is the number of total layers of the laminated conical shell, $Q_{ij}^{(k)}$, the element of the transformed reduced stiffness matrix for the kth layer, and h_k and h_{k-1} denote distances from the shell reference surface to the outer and inner surfaces of the kth layer. By substituting Eq. (14) into Eqs. (1)–(3), governing equations for the linear free vibration analysis of composite laminated conical shells are obtained:

$$L_{11}u + L_{12}v + L_{13}w - \rho h\frac{\partial^2 u}{\partial t^2} = 0, \tag{18a}$$

$$L_{21}u + L_{22}v + L_{23}w - \rho h\frac{\partial^2 v}{\partial t^2} = 0, \tag{18b}$$

$$L_{31}u + L_{32}v + L_{33}w - \rho h\frac{\partial^2 w}{\partial t^2} = 0, \tag{18c}$$

where L_{ij} are the differential operators. These are given in Appendix A. The displacement terms are taken as

$$u = U(x)\cdot\cos(n\theta)\cdot\cos(\omega t), \tag{19a}$$

$$v = V(x)\cdot\sin(n\theta)\cdot\cos(\omega t), \tag{19b}$$

$$w = W(x)\cdot\cos(n\theta)\cdot\cos(\omega t). \tag{19c}$$

Substituting Eqs. (19) into Eqs. (18), the governing equations can be written as

$$G_{111}U + G_{112}\frac{\partial U}{\partial x} + G_{113}\frac{\partial^2 U}{\partial x^2} + G_{121}V + G_{122}\frac{\partial V}{\partial x} + G_{131}W + G_{132}\frac{\partial W}{\partial x} + G_{133}\frac{\partial^2 W}{\partial x^2} + G_{134}\frac{\partial^3 W}{\partial x^3} = -\rho h\omega^2 U, \tag{20}$$

$$G_{211}U + G_{212}\frac{\partial U}{\partial x} + G_{221}V + G_{222}\frac{\partial V}{\partial x} + G_{223}\frac{\partial^2 V}{\partial x^2} + G_{231}W + G_{232}\frac{\partial W}{\partial x} = -\rho h\omega^2 V, \tag{21}$$

$$G_{311}U + G_{312}\frac{\partial U}{\partial x} + G_{313}\frac{\partial^2 U}{\partial x^2} + G_{314}\frac{\partial^3 U}{\partial x^3} + G_{321}V + G_{322}\frac{\partial V}{\partial x} + G_{323}\frac{\partial^2 V}{\partial x^2} + G_{331}W + G_{332}\frac{\partial W}{\partial x} + G_{333}\frac{\partial^2 W}{\partial x^2} + G_{334}\frac{\partial^3 W}{\partial x^3} + G_{335}\frac{\partial^4 W}{\partial x^4} = -\rho h\omega^2 W, \tag{22}$$

where G_{ijk} are the constant coefficients defined in Appendix B. In this study, the following three type main boundary conditions and four subclasses boundary conditions for clamped edge are considered. These are defined as

Simply supported edge (S):

$$V = 0, \quad W = 0, \quad N_x = 0, \quad M_x = 0. \tag{23a}$$

Clamped edge (C):

$$U = 0, \quad V = 0, \quad W = 0 \quad \text{and} \quad W_x = 0. \tag{23b}$$

Free edge (F):

$$V_x = 0, \quad M_x = 0, \quad N_x = 0, \quad S_{x\theta} = 0. \tag{23c}$$

Type-1 *Clamped boundary* (C–C1):

$$W = 0, \quad N_x = 0, \quad N_{x\theta} = 0, \quad W_x = 0. \tag{23d}$$

Type-2 *Clamped boundary* (C–C2):

$$W = 0, \quad U = 0, \quad N_{x\theta} = 0, \quad W_x = 0. \tag{23e}$$

Type-3 *Clamped boundary* (C–C3):

$$W = 0, \quad V = 0, \quad N_x = 0, \quad W_x = 0. \tag{23f}$$

Type-4 *Clamped boundary* (C–C4):

$$U = 0, \quad V = 0, \quad W = 0, \quad W_x = 0. \tag{23g}$$

Wei et al. [51] and Zhao and Wei [58] proposed a practical method to incorporate the boundary conditions. More recently, Zhao et al. [57] applied the iteratively matched boundary method to impose the free boundary conditions for solid mechanic problem.

3. Discrete singular convolution (DSC)

Discrete singular convolutions (DSC) algorithm introduced by Wei [43] in 1999. As stated by Wei [47,48,45] singular convolutions (SC) are a special class of mathematical transformations, which appear in many science and engineering problems, such as the Hilbert, Abel and Radon transforms. In fact, these transforms are essential to many practical applications, such as computational electromagnetics, signal and image processing, pattern recognition, tomography, molecular potential surface generation and dynamic simulation. It is the most convenient way to discuss the singular convolution in the context of the theory of distributions. It not only provides a rigorous justification for a number of informal manipulations in physical science and engineering, but also opens a new area of mathematics, which in turn gives impetus in many other mathematical disciplines, such as operator calculus, differential equations, functional analysis, harmonic analysis and transformation theory [48,49]. In fact, the theory of wavelets and frames, a new mathematical branch developed in recent years, can also find its root in the theory of distributions [44].

Wei and his co-workers first applied the DSC algorithm to solve solid and fluid mechanics problem [52,53,46,50]. Zhao et al. [59,60] analyzed the high-frequency vibration of plates and plate vibration under irregular internal support using DSC algorithm. Zhao and Wei [58] adopted the DSC in the vibration analysis of rectangular plates with nonuniform boundary conditions. Numerical solution of unsteady incompressible flows using DSC is given by Wan et al. [42]. A good comparative accuracy of DSC and generalized differential quadrature methods for vibration analysis of rectangular plates is presented by Ng et al. [31]. Yunshan [56] presented the DSC-Ritz method for the free vibration analysis of Mindlin plates.

More recently, Lim et al. [23] proposed the DSC-Ritz method for high-mode frequency analysis of thick shallow shells. It is emphasized that the DSC algorithm work very well for the vibration analysis of plates, especially for high-frequency analysis of plates and shells. Furthermore, it is also concluded that the DSC algorithm has global methods' accuracy and local methods' flexibility for solving differential equations in applied mechanics. The mathematical foundation of the DSC algorithm is the theory of distributions and wavelet analysis. Consider a distribution, T and $\eta(t)$ as an element of the space of the test function. A singular convolution can be defined by

$$F(t) = (T * \eta)(t) = \int_{-\infty}^{\infty} T(t - x)\eta(x)\,\mathrm{d}x, \tag{24}$$

where $T(t-x)$ is a singular kernel. For example, singular kernels of delta type

$$T(x) = \delta^{(n)}(x), \quad (n = 0, 1, 2, \ldots,). \tag{25}$$

Kernel $T(x) = \delta(x)$ is important for interpolation of surfaces and curves, and $T(x) = \delta^{(n)}(x)$ for $n > 1$ are essential for numerically solving differential equations. Since these kernels are singular, they are not suitable for directly digitized in computers. In order to avoid this difficulty, Wei [43] suggested a new form for sequence of approximations (T_α) of the distribution T as

$$\lim_{\alpha \to \alpha_0} T_\alpha(x) \to T(x), \tag{26}$$

in which α_0 is a generalized limit. With a sufficiently smooth approximation, it is more effective to consider a discrete singular convolution

$$F_\alpha(t) = \sum_k T_\alpha(t - x_k) f(x_k), \tag{27}$$

where $F_\alpha(t)$ is an approximation to $F(t)$ and $\{x_k\}$ is an appropriate set of discrete points on which the DSC (24) is well defined.

3.1. Regularized Shannon's delta kernel (RSDK)

More recently, the use of some new kernels and regularizer such as delta regularizer [47] was proposed to solve applied mechanics problem. The Shannon's kernel is regularized as

$$\delta_{\Delta,\sigma}(x - x_k) = \frac{\sin[(\pi/\Delta)(x - x_k)]}{(\pi/\Delta)(x - x_k)} \exp\left[-\frac{(x - x_k)^2}{2\sigma^2}\right], \quad \sigma > 0, \tag{28}$$

where Δ is the grid spacing. It is also known that the truncation error is very small due to the use of the Gaussian regularizer, the above formulation given by Eq. (28) is practically and has an essentially compact support for numerical interpolation. In fact, Shannon's delta sequence kernel can be derived from the generalized Lagrange interpolation formula

$$S_k(x) = \frac{G(x)}{G'(x_k)(x - x_k)}, \tag{29}$$

where $G(x)$ is an entire function given by

$$G(x) = (x - x_0) \prod_{k=1}^{\infty} \left(1 - \frac{x}{x_k}\right)\left(1 - \frac{x}{x_{-k}}\right) \tag{30}$$

and G' denotes the derivatives of G. If $\{x_k\}_{k \in Z}$ are limited to a set of points on a uniform infinite grid ($x_k = k\Delta = -x_{-k}$), Eq. (30) can be simplified

$$G(x) = x \prod_{k=-\infty, k\neq 0}^{\infty} \left(1 - \frac{x}{k\Delta}\right) = x \prod_{k=1}^{\infty} \left(1 - \frac{x^2}{k^2\Delta^2}\right) = \Delta \frac{\sin[(\pi/\Delta)x]}{\pi}. \tag{31}$$

Since $G'(x_k)$ reduced to $G'(x_k) = (-1)^k$ for uniform grid, Eq. (31) gives rise to

$$S_k(x) = \frac{G(x)}{G'(x_k)(x - x_k)} = \frac{(-1)^k \sin[(\pi/\Delta)x]}{(\pi/\Delta)(x - k\Delta)} = \frac{\sin[(\pi/\Delta)(x - x_k)]}{(\pi/\Delta)(x - x_k)}, \tag{32}$$

Eq. (28) can also be used to provide discrete approximations to the singular convolution kernels of the delta type

$$f^{(n)}(x) \approx \sum_{k=-M}^{M} \delta_{\alpha,\sigma}^{(n)}(x - x_k) f(x_k), \quad (n = 0, 1, 2, \ldots,) \tag{33}$$

or

$$f^{(n)}(x) \approx \sum_{k=-M}^{M} \delta_{\Delta}(x - x_k) f(x_k), \tag{34}$$

where $\delta_{\Delta}(x - x_k) = \Delta\delta_{\alpha}(x - x_k)$ and superscript (n) denotes the nth-order derivative, and $2M + 1$ is the computational bandwidth which is centered around x and is usually smaller than the whole computational domain. When the regularized Shannon's delta kernel (RSDK) is used, the detailed expressions for $\delta_{\Delta,\sigma}(x)$, $\delta_{\Delta,\sigma}^{(1)}(x)$, $\delta_{\Delta,\sigma}^{(2)}(x)$, $\delta_{\Delta,\sigma}^{(3)}(x)$ and $\delta_{\Delta,\sigma}^{(4)}(x)$ can be easily obtained. Detailed formulations on these coefficients are found in [23,43,47]. First-order derivative, for example, are given as

$$\begin{aligned}\delta_{\pi/\Delta,\sigma}^{(1)}(x_m - x_k) = {} & \frac{\cos(\pi/\Delta)(x - x_k)}{(x - x_k)} \exp[-(x - x_k)^2/2\sigma^2] - \frac{\sin(\pi/\Delta)(x - x_k)}{\pi(x - x_k)^2/\Delta} \exp[-(x - x_k)^2/2\sigma^2)] \\ & - \frac{\sin(\pi/\Delta)(x - x_k)}{(\pi\sigma^2/\Delta)} \exp[-(x - x_k)^2/2\sigma^2)].\end{aligned} \tag{35}$$

In this stage, consider an operator O having a differential part D and a function part of F:

$$O = D + F. \tag{36}$$

In the DSC approach, it is convenient to choose a grid representation for the coordinate so that the function part of F of the operator is diagonal. Hence, its discretization is simply given by a direct interpolation on the grid

$$F(x) \to F(x_k)\delta_{m,k}. \tag{37}$$

For solution of differential equations, approximation to derivatives is required. Such approximation can be constructed by using DSC kernels of the delta type with $n \neq 0$. Let us consider a one dimensional, nth order DSC kernel of delta type

$$\delta_{\sigma,\Delta}^{(n)}(x - x_k), \quad (n = 0, 1, 2, \ldots,). \tag{38}$$

Here $\delta_{\sigma,\Delta}^{(0)}(x - x_k) = \delta_{\sigma,\Delta}(x - x_k)$ is the DSC kernel described in Eq. (34). The differential part of the operator on the coordinate grid is then represented by functional derivatives

$$D = \sum_{n=1} d_n(x) \frac{d^n}{\mathrm{d}x^n} \to \sum_{n=1} d_n(x_m)\delta_{\alpha,\sigma}^{(n)}(x_m - x_k), \tag{39}$$

where $d_n(x)$ is a coefficient and $\delta_{\alpha,\sigma}^{(n)}(x_m - x_k)$ is analytically given by

$$\delta_{\alpha,\sigma}^{(n)}(x_m - x_k) = \left[\left(\frac{\mathrm{d}}{\mathrm{d}x}\right)^n \delta_{\alpha,\sigma}(x_m - x_k)\right]_{x=x_m}. \tag{40}$$

Thus, the full DSC-matrix representation for the operator, O, is given by [47]

$$O(x_m - x_k) = \sum_{n} d_n(x_m)\delta_{\alpha,\sigma}^{(n)}(x_m - x_k) + F(x_m)\delta_{m,k}. \tag{41}$$

To approximate the derivative of a given function with respect to a space variable at a given discrete point, the DSC is usually uses a weighted linear combination of the function values at $2M + 1$ points (M points to the left and M points

to the right) in the direction of the space variable, where M is the known as the half bandwidth. The nth derivative of a function $f(x)$ at the ith point, x_i, is then approximated as

$$f^{(n)}(x_i) \approx \sum_{j=-M}^{M} W_{i,j}^{(n)} f(x_{i+j}); \quad i = 0, 1, \ldots, N-1, \tag{42}$$

where $W_{i,j}^{(n)}$ can be obtained using the some known DSC kernels. Therefore, the discretized forms of Eqs. (23)

$$\begin{aligned} &G_{111}U_{i,j} + G_{112}\sum_{k=-M}^{M}\delta_{\Delta,\sigma}^{(1)}(k\Delta x)U_{i+k,j} + G_{113}\sum_{k=-M}^{M}\delta_{\Delta,\sigma}^{(2)}(k\Delta x)U_{i+k,j} + G_{121}V_{i,j} \\ &\quad + G_{122}\sum_{k=-M}^{M}\delta_{\Delta,\sigma}^{(1)}(k\Delta x)V_{i,j+k} + G_{131}W_{i,j} + G_{132}\sum_{k=-M}^{M}\delta_{\Delta,\sigma}^{(1)}(k\Delta x)W_{i,j+k} = -\rho h\omega^2 U_{i,j}, \end{aligned} \tag{43a}$$

$$\begin{aligned} &G_{211}U_{i,j} + G_{212}\sum_{k=-M}^{M}\delta_{\Delta,\sigma}^{(1)}(k\Delta x)U_{i+k,j} + G_{221}V_{i,j} + G_{122}\sum_{k=-M}^{M}\delta_{\Delta,\sigma}^{(1)}(k\Delta x)V_{i,j+k} + G_{223}\sum_{k=-M}^{M}\delta_{\Delta,\sigma}^{(2)} \\ &\quad \times (k\Delta x)V_{i+k,j} + G_{231}W_{i,j} + G_{232}\sum_{k=-M}^{M}\delta_{\Delta,\sigma}^{(1)}(k\Delta x)W_{i,j+k} + G_{233}\sum_{k=-M}^{M}\delta_{\Delta,\sigma}^{(2)}(k\Delta x)W_{i+k,j} = -\rho h\omega^2 V_{i,j}, \end{aligned} \tag{43b}$$

$$\begin{aligned} &G_{311}U_{i,j} + G_{312}\sum_{k=-M}^{M}\delta_{\Delta,\sigma}^{(1)}(k\Delta x)U_{i+k,j} + G_{321}V_{i,j} + G_{322}\sum_{k=-M}^{M}\delta_{\Delta,\sigma}^{(1)}(k\Delta x)V_{i,j+k} \\ &\quad + G_{323}\sum_{k=-M}^{M}\delta_{\Delta,\sigma}^{(2)}(k\Delta x)V_{i+k,j} + G_{331}W_{i,j} + G_{332}\sum_{k=-M}^{M}\delta_{\Delta,\sigma}^{(1)}(k\Delta x)W_{i,j+k} \\ &\quad + G_{333}\sum_{k=-M}^{M}\delta_{\Delta,\sigma}^{(2)}(k\Delta x)W_{i+k,j} + G_{334}\sum_{k=-M}^{M}\delta_{\Delta,\sigma}^{(3)}(k\Delta x)W_{i+k,j} \\ &\quad + G_{335}\sum_{k=-M}^{M}\delta_{\Delta,\sigma}^{(4)}(k\Delta x)W_{i+k,j} = -\rho h\omega^2 W_{i,j}, \end{aligned} \tag{43c}$$

where $\delta_{\alpha,\sigma}^{(n)}$ is the coefficients of the regualrized Shannon's kernel, given in Eq. (38). Thus, the governing equations are spatially discretized by using the DSC algorithm. From the above procedures, one can derive the general form of eignvalue equation as follows:

$$GU = \Omega BU, \tag{44}$$

where U is the displacement vector defined as follows:

$$U = [U_{ijk} \;\; V_{ijk} \;\; W_{ijk}]^{\mathrm{T}}. \tag{45}$$

In Eq. (44), G and B are the matrices derived from the governing equations described by (43), and the boundary conditions considered in Eq. (23). In the above eigenvalue equation, W is the nondimensional frequency parameter.

4. Numerical applications

The utility and robustness of the proposed method is illustrated by a number of numerical examples in this section. In order to simplify the presentation S, F, and C represent simply supported, free, and clamped supports, respectively.

Table 1
Comparison of fundamental frequency parameters of annular isotropic plates

Boundary conditions	R_1/R_2	HDQ (present study ($N=15$))	FEM Ref. [4] ($N=18$)	Leissa Ref. [15]	DSC			
					$N=9$	$N=11$	$N=16$	$N=21$
S–S	0.1	14.42	14.38	14.44	19.36	15.61	14.50	14.48
	0.2	16.89	17.11	17.39	23.85	16.78	17.41	17.38
	0.3	21.24	20.84	21.10	26.32	23.54	21.07	21.06
C–S	0.1	17.76	18.01	17.85	24.11	19.26	17.86	17.86
	0.2	22.81	23.42	22.79	28.74	23.99	22.80	22.78
	0.3	29.98	31.17	30.05	36.03	32.73	30.06	30.06

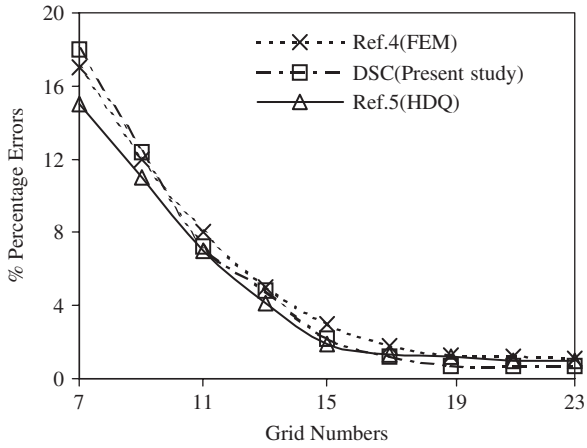

Fig. 2. Comparison of percentage errors with grid numbers for different approach.

In this section some numerical results are presented for the free vibration analysis of isotropic, orthotropic, and laminated conical and cylindrical shells with different geometric and material parameters under different boundary conditions. Free vibrations of annular isotopic plates are treated as special cases.

4.1. Numerical results for annular plates ($\alpha = \pi/2$)

To check whether the purposed formulation and programming are correct, an isotropic annular plate is analyzed first. In Table 1, the DSC results are compared with those given by Leissa [15] and Civalek [4] for isotropic annular plates. The DSC results were obtained 16 grid points. It can be seen from the table that, the present DSC results agree very well with those of Leissa [15]. By comparing with the results of Leissa [15], the DSC results using 16 uniform grid points are very accurate. When the number of grid points is larger than 16, the DSC results are independent of grid. The results given by Civalek [4] are also listed in this table. The results given by Civalek [4] are obtained using the finite element method (FEM). From Table 1, it is shown that the convergence of DSC results is very good for only 16 grid points. The DSC results are generally in agreement with the results produced from the harmonic differential quadrature (HDQ) [5] and finite element method (FEM) [4]. The FEM results are found using the program developed by Civalek [4]. The present numerical solutions are in close agreement with the HDQ [5], FEM [4] and analytical solutions [15] available in the literature. The percentage errors of the frequencies between the DSC and the references data of Leissa [15] are displayed in Fig. 2. The variation of the error with the number of grid points was also shown in Fig. 2 for the HDQ and FEM methods. For comparison purpose the HDQ solution also obtained by author using the computer program developed by author in her Ph.D. thesis is used [25]. It was found that as the number of grid points increases, the percentage error is decreases. However, a reasonably converged solution may be achieved for $M=16$. It is observed

Table 2
Frequency parameters of S–S cylindrical shells ($h/R = 0.002$)

n	$L/R = 1$			$L/R = 5$		
	Ref. [14]	Ref. [20]	Present	Ref. [14]	Ref. [20]	Present
1	1.061284	1.061284	1.061283	0.248635	0.268635	0.268633
2	0.804054	0.804052	0.804052	0.107203	0.107202	0.107200
3	0.598331	0.598327	0.598328	0.055087	0.055086	0.055085
4	0.450144	0.450138	0.450141	0.033790	0.033786	0.033788
5	0.345253	0.345244	0.345246	0.025794	0.033786	0.033792
6	0.270754	0.270742	0.270753	0.025877	0.025872	0.025878

that by increasing the number of grid points within the range $9 \leqslant M \leqslant 21$, the DSC results approach monotonically the corresponding Leissa [15] results. The known boundary conditions are easily incorporated in the DSC as well as the other numerical methods such as HDQ. A good comparative accuracy of differential quadrature (DQ) and DSC methods for vibration analysis of plates is presented by Ng et al. [31]. More detailed information can be found in this reference.

4.2. Numerical results for isotropic cylindrical shells

To validate the purposed approach, comparisons of DSC results with available published data were made for isotropic cylindrical shell. The present analysis is applicable to laminated cylindrical shells by letting $\alpha = 0$ in the relevant formulation. The numerical results for the laminated cylindrical shells are given by the dimensionless frequency parameter λ. This parameter is given by

$$\lambda = 2\pi R\sqrt{\frac{\rho h}{A_{11}}}\omega,$$

where ω is referred to as the frequency parameter. In the first test example, the free vibration of cylindrical shells is considered. S–S boundary conditions are taken into account. Results are presented in Table 2. Results from the present DSC method are compared with the results of Lam and Loy [14] and Liew et al. [20]. It is seen that the frequencies obtained by the DSC method are in good agreement with the analytical and numerical solutions in the literature.

The relationship between the frequency parameter Ω and circumferential wave number n are shown in Fig. 3. The results are presented for four different boundary conditions. The frequency parameter Ω first decreases rapidly ($n \leqslant 4$) and then increases with increasing circumferential wave number n ($n > 4$). The C–C cylindrical shell has the highest frequency parameter Ω, followed by the S–C, S–S, and C–F shells. It is shown that, the differences amongst the frequency parameters of the three boundary conditions are large for smaller circumferential wave number n ($n \leqslant 6$). In other words, the effect of boundary conditions is significant for small circumferential wave number. With the increase of circumferential wave number n ($n > 6$), the effect of the boundary conditions on the frequency parameter is insignificant.

4.3. Numerical results for isotopic conical shells

Table 3 shows the convergence of computed frequency parameters Ω for an isotropic F–S conical shell with $L \sin\theta/R_2 = 0.75$, $h/R_2 = 0.01$ for two different cone angle. From Table 3, it is shown that the convergence of DSC results is very good. By comparing with the results of Irie et al. [10], the DSC results are very accurate. It is observed that a good agreement between the present calculated results and the results of literature [10,5] has been obtained. Effect of the $L \sin\alpha/R_2$ ratio on frequencies of conical shells for different cone angles are show in Fig. 4. With the increase of cone angle, frequency parameter Ω increases gradually. Influence of cone angles is significant at small r ratio.

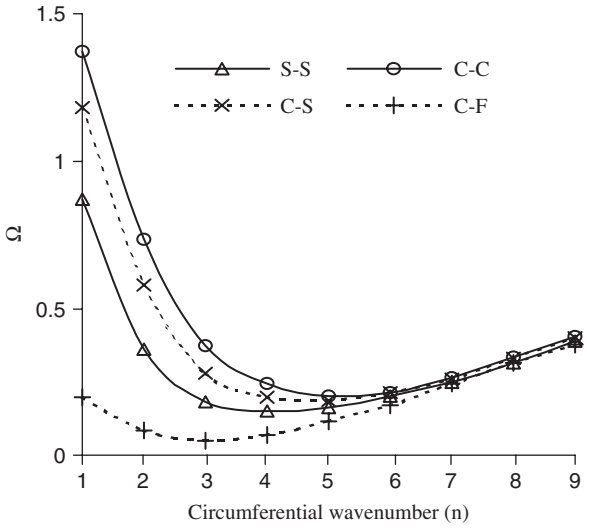

Fig. 3. Variation of backward-wave frequency parameter Ω with the circumferential wave number n for cylindrical shells ($h/R = 0.002$; $L/R = 6$).

Table 3
Frequency parameters of F–S conical shells ($v = 0.3$, $h/R_2 = 0.01$)

Circumferential wave number (n)	$L \sin \alpha/R_2 = 0.75$					
	$\alpha = 30°$			$\alpha = 60°$		
	Present DSC	HDQ Ref. [5]	Ref. [10]	Present DSC	HDQ Ref. [5]	Ref. [10]
0	0.0875	0.0876	0.0877	0.1370	0.1372	0.1369
1	0.0761	0.0761	0.0762	0.1790	0.1788	0.1787
2	0.0780	0.0782	0.0779	0.1491	0.1490	0.1489
3	0.1553	0.1555	0.1551	0.1945	0.1947	0.1946
4	0.1918	0.1919	0.1917	0.2408	0.2410	0.2408
5	0.2182	0.2183	0.2181	0.2690	0.2691	0.2691
6	0.2542	0.2544	0.2543	0.3089	0.3090	0.3088
7	0.2997	0.3001	0.2995	0.3614	0.3615	0.3614
8	0.3532	0.3533	0.3533	0.4251	0.4253	0.4250
9	0.4155	0.4154	0.4153	0.4981	0.4983	0.4982

4.4. Numerical results for laminated cylindrical shells

The present analysis can be applied to the laminated cylindrical shells by letting $R_1 = R_2$ in Fig. 1. In other words, by holding the value of R_1 and vanishing the value of α, the conical shell will degenerate to a cylindrical shell. So, the present analysis is applicable to laminated cylindrical shells by letting $\alpha = 0$ in the relevant formulation. The elementary material parameters of each layer are given as: $v_{12} = 0.25$, $v_{22} = 0.3$, $E_{11}/E_{22} = 40$, $G_{12}/E_{22} = 0.5$, where subscripts 1 and 2 denote the directions parallel and transverse to the fiber direction, respectively. Since there is an infinite complexity of the class of cross-ply laminates, only a regular antisymmetric cross-ply laminated shell is considered in this example. For this type of laminated composite, the coefficients in Eqs. (17) can be simplified as:

$$A_{11} = A_{22} = h(Q_{11} + Q_{22})/2, \quad A_{12} = Q_{12}h, \quad A_{66} = Q_{66}h,$$

$$B_{11} = -B_{22} = h^2(Q_{11} - Q_{22})/4N_L, \quad B_{11} = 0, \quad B_{66} = 0,$$

$$D_{11} = B_{22} = h^3(Q_{11} + Q_{22})/24, \quad D_{12} = h^3(Q_{12})/12, \quad D_{66} = h^3(Q_{66})/12.$$

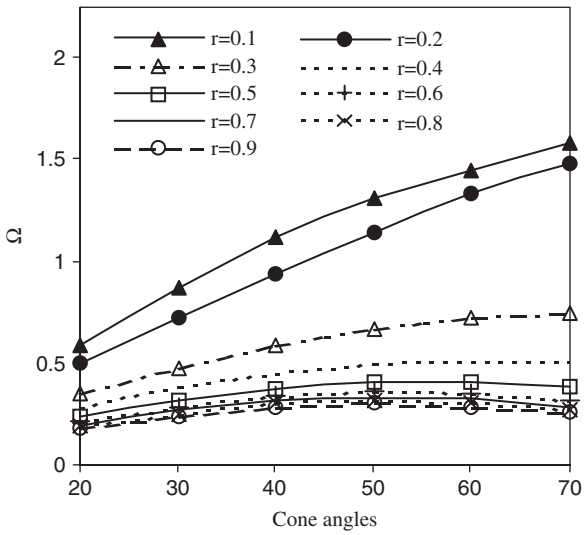

Fig. 4. Effect of the $L \sin \alpha / R_2$ ratio on frequencies of conical shells for different cone angles ($h/R_2 = 0.01$).

Table 4
Fundamental frequency parameters of an antisymmetric cross-ply laminated cylindrical shell with the S–C boundary condition ($v = 0.3$, $h/R_2 = 0.01$)

h/R	L/R	Present DSC results		CST Ref. [35]		DQM Ref. [54]	
		Maximum coupling $N_L = 2$	Without coupling ($N_L = \infty$)	Maximum coupling $N_L = 2$	Without coupling ($N_L = \infty$)	Maximum coupling $N_L = 2$	Without coupling ($N_L = \infty$)
0.01	1	0.6585	0.7729	0.6440	0.8044	0.6725	0.8003
	2	0.3802	0.4463	0.3750	0.4545	0.3742	0.4534
	5	0.1849	0.2186	0.1858	0.2193	0.1852	0.2187
	10	0.1014	0.1195	0.1030	0.1223	0.1027	0.1217
	20	0.0477	0.0628	0.0496	0.0641	0.0494	0.0639
0.02	1	0.8002	0.9803	0.8557	1.0944	–	–
	2	0.4604	0.5584	0.4764	0.5769	–	–
	5	0.2191	0.2715	0.2293	0.2752	–	–
	10	0.1111	0.1429	0.1238	0.1487	–	–
	20	0.0632	0.0632	0.0683	0.0886	–	–
0.05	1	1.1406	1.4803	1. 3201	1.8327	1.2820	1.6531
	2	0.6228	0.7474	0.6518	0.8146	0.6432	0.7975
	5	0.2785	0.3502	0.2886	0.3615	0.2876	0.3562
	10	0.1663	0.1956	0.1745	0.2021	0.1733	0.2015
	20	0.0771	0.0787	0.0875	0.0886	0.0870	0.0881

For the antisymmetric cross-ply laminates, the extension–bending coupling terms reach their maximum values with two layers ($N_L = 2$) and become zero with an infinite number of layers ($N_L = \infty$). The fundamental frequency parameters λ for an antisymmetric cross-ply laminated circular cylindrical shell with the S–C boundary condition are shown in Table 4. This table shows the fundamental frequency parameters based on the classical shell theory (CST) [35] and present DSC formulation. The results given by Wu and Wu [54] are also listed in this table for the purpose of comparison. Wu and Wu [54] used the differential quadrature method (DQM) in their study. The present numerical solutions are in close agreement with the DQM and CST solutions available in the literature. It is also shown from these results given in Table 4 that the results of two layers ($N_L = 2$) are always less than that of infinite layers ($N_L = \infty$). As a consequence, it may be concluded that the fundamental frequency parameters decrease as the coupling rigidity terms increase.

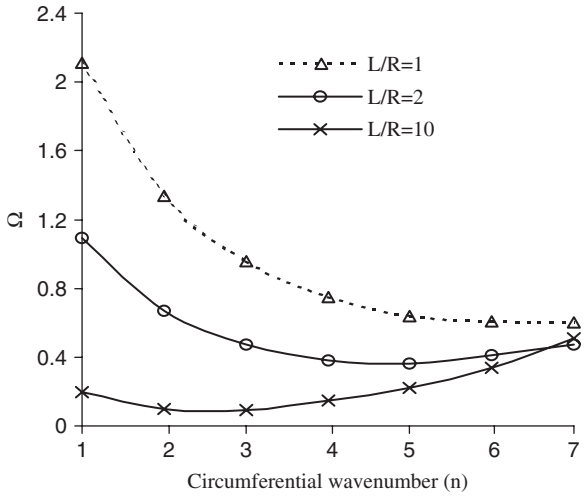

Fig. 5. Variation of frequency parameter Ω with the circumferential wave number n for an antisymmetric crossply laminated shell with S–S boundary conditions ($h/R = 0.01$).

Table 5
Fundamental frequency parameters of an antisymmetric cross-plied laminated conical shell with the S–S boundary condition ($\alpha = 30$, $L \sin \alpha / R_2 = 0.25$)

h/R_2	Present DSC results		Tong [41]		GDQ [33]	
	Maximum coupling $N_L = 2$	Without coupling ($N_L = \infty$)	Maximum coupling $N_L = 2$	Without coupling ($N_L = \infty$)	Maximum coupling $N_L = 2$	Without coupling ($N_L = \infty$)
0.01	0.1785	0.1980	0.1769	0.1978	0.1799	0.1976
0.02	0.2128	0.2353	0.2119	0.2355	0.2153	0.2351
0.03	0.2402	0.2671	0.2360	0.2671	0.2397	0.2667
0.04	0.2607	0.2994	0.2578	0.2992	0.2620	0.2987
0.05	0.2816	0.3307	0.2794	0.3308	0.2841	0.3303
0.06	0.3024	0.3611	0.3010	0.3606	0.3061	0.3602

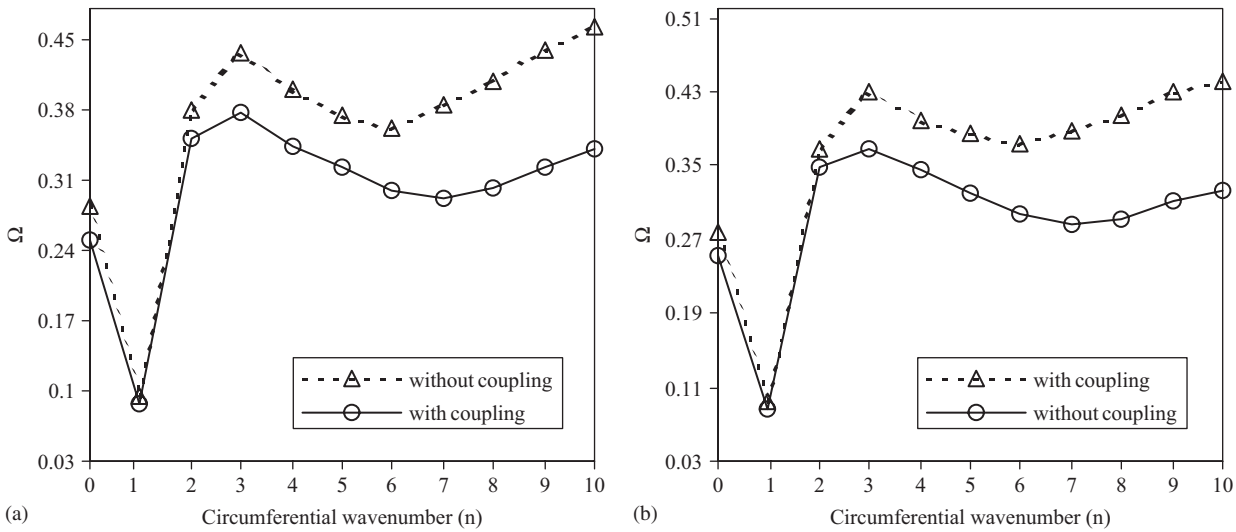

Fig. 6. Effect of extension–bending coupling on frequency parameter for C–C1 conical shells: (a) $\alpha = 30°$; (b) 45°.

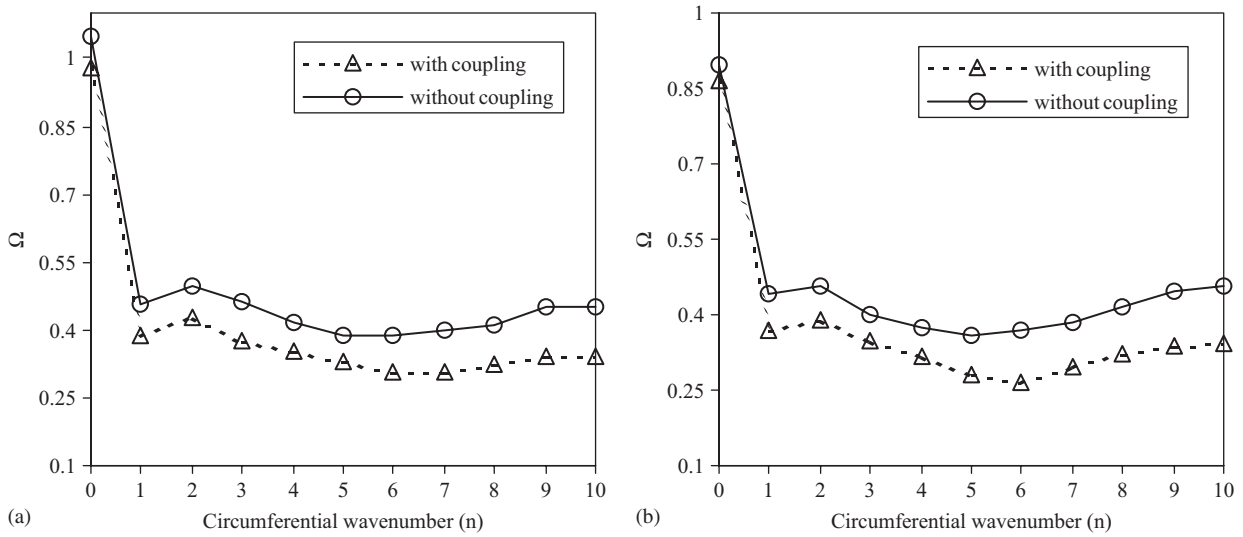

Fig. 7. Effect of extension–bending coupling on frequency parameter for C–C2 conical shells: (a) $\alpha = 30°$; (b) 45°.

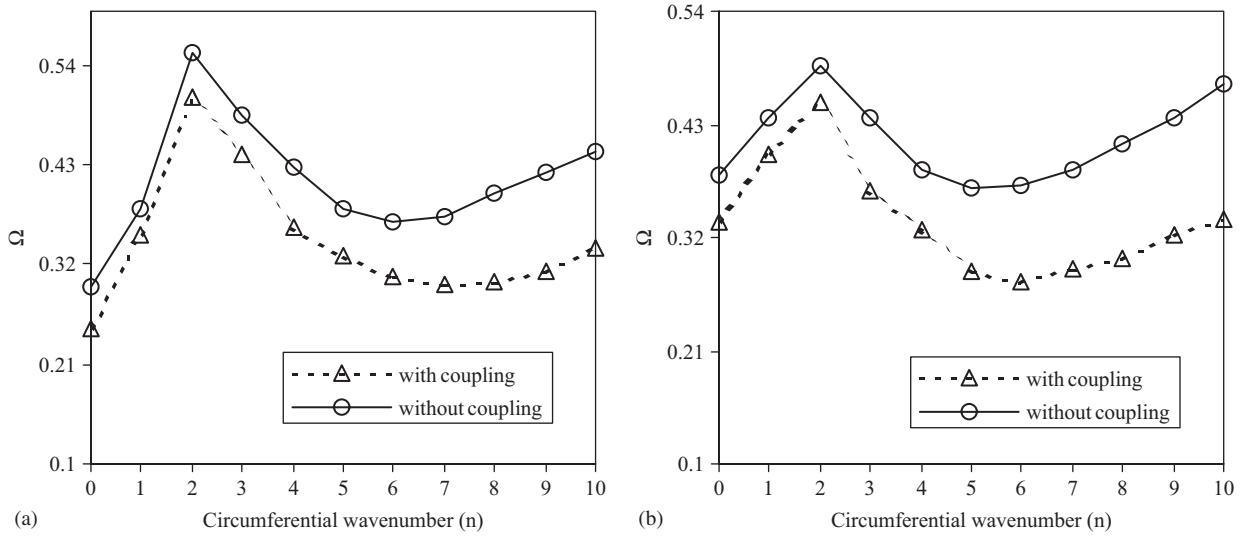

Fig. 8. Effect of extension–bending coupling on frequency parameter for C–C3 conical shells: (a) $\alpha = 30°$; (b) 45°.

The variation of the frequency parameter Ω; with L/R ratio is shown in Fig. 5. It is concluded that from these figures, the frequency parameter is uniformly decrease when the ratio L/R increases.

4.5. Numerical results for orthotropic laminated conical shells

It is noted that the extension bending coupling terms reach their maximum values with two plies ($N_L = 2$) and become zero with an infinite number of plies ($N_L = \infty$). Thus the case of $N_L = 2$ is referred to as "maximum coupling" and the case of $N_L = \infty$ is referred to as "without coupling". The fundamental frequency parameters λ for an antisymmetric cross-plied laminated conical shell with the S–S boundary condition are shown in Table 5. A detailed comparison between the differential quadrature results [33] and those of Tong [41] for various h/R_2 ratios is listed in this table. It may be concluded that increasing the h/R_2 ratio will always result in increased frequency. It is also shown that the

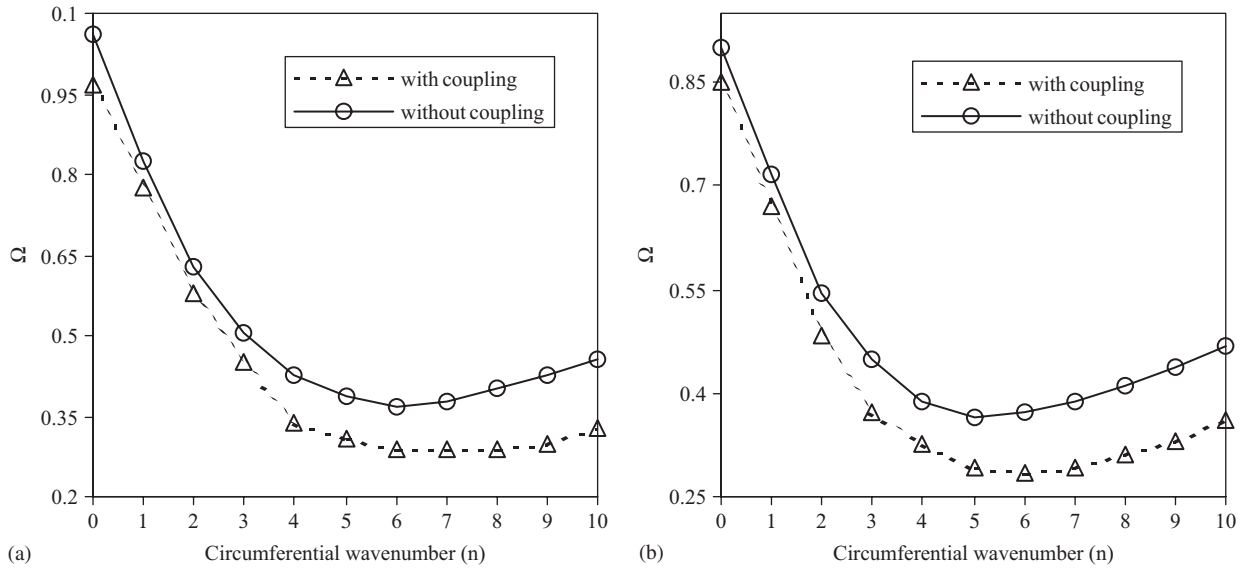

Fig. 9. Effect of extension–bending coupling on frequency parameter for C–C4 conical shells: (a) $\alpha = 30°$; (b) 45°.

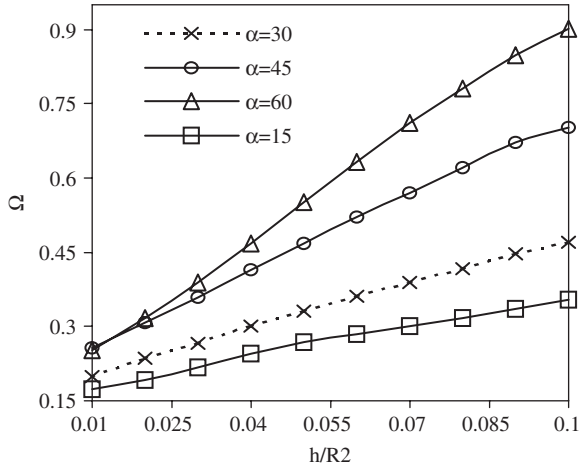

Fig. 10. Variation of frequency versus geometric ratio h/R_2 for various cone angles of S–S conical shell ($L/R_2 = 0.5$; $h/R_2 = 0.01$; $\nu = 0.3$).

frequency parameters of two layers ($N_L = 2$) are always less than that of infinite layers ($N_L = \infty$). As a consequence, it may be concluded that the fundamental frequency parameters decrease as the coupling rigidity terms increase.

The effect of extension-bending coupling on frequency response with circumferential wave number is shown in Figs. 6–9 for antisymmetric cross-ply laminated conical shell. Two different semivertex angles such as 30° and 45° and four different boundary conditions are taken into consideration. It is shown that the frequency parameters of infinite layers ($N_L = \infty$) are always greater than that of two layers ($N_L = 2$). It is concluded that, the values of frequencies for the four classes of boundary conditions rank consecutively in the following sequence C–C4>C–C2>C–C1>C–C3. It is also observed that the frequency parameters under the C–C1 boundary conditions are nearly equal to that under C–C3. Similarly, the frequency parameters under the C–C2 boundary conditions are nearly equal to that under C–C4. Furthermore, the extension–bending coupling becomes large as the circumferential wavenumber increases.

For ratio $L/R_2 = 0.5$, the influence of geometric ratio h/R_2 on the relation between frequency parameter Ω is shown in Fig. 10 for four different cone angle, α. It can be concluded that the influence of h/R_2 ratio on the relation between

frequency parameter Ω and the cone angle is significant. It is shown that the increasing value of α always increases the frequency parameter Ω. It is also observed that the influence of boundary condition on the frequency parameter Ω with h/R_2 is significant.

5. Conclusions

The numerical solution of partial differential equations plays a considerable role in the areas of engineering. Therefore, an effective numerical technique for the solution of partial equations is very desirable. In seeking a more efficient numerical method that requires fewer grid points yet achieves acceptable accuracy, the method of DSC was introduced by Wei [43].

The work presented here concerns the use of DSC method for the vibration analysis of laminated conical and cylindrical shells. Results were compared with existing solutions showing excellent performance. It is found that the convergence of DSC approach is very good and the results agree well with those obtained by other researchers. Thus, the DSC method provides an accurate, efficient means of solving problems for orthotropic laminated conical and cylindrical shells.

Acknowledgements

The financial support of the Scientific Research Projects Unit of Akdeniz University is gratefully acknowledged.

Appendix A

Differential operators L_{ij} in Eqs. (18) are defined as follows:

$$L_{11} = A_{11}\frac{\partial^2}{\partial x^2} + A_{11}\frac{\sin\alpha}{R(x)}\frac{\partial}{\partial x} - A_{22}\frac{\sin^2\alpha}{R^2(x)} + \frac{A_{66}}{R^2(x)}\frac{\partial^2}{\partial\theta^2},$$

$$L_{12} = \frac{(A_{12}+A_{66})}{R(x)}\frac{\partial^2}{\partial x\partial\theta} - \frac{(A_{22}+A_{66})\sin\alpha}{R^2(x)}\frac{\partial}{\partial\theta} + \frac{(B_{12}+2B_{66})\cos\alpha}{R^2(x)}\frac{\partial^2}{\partial x\partial\theta} + \frac{(B_{12}+B_{22}+2B_{66})\sin\alpha\cos\alpha}{R(x)}\frac{\partial}{\partial\theta},$$

$$L_{13} = A_{12}\frac{\cos\alpha}{R(x)}\frac{\partial}{\partial x} - A_{22}\frac{\sin\alpha\cos\alpha}{R^2(x)} - B_{11}\frac{\partial^3}{\partial x^3} - \frac{(B_{12}+2B_{66})\cos\alpha}{R^2(x)}\frac{\partial^3}{\partial x\partial\theta^2} - B_{11}\frac{\sin\alpha}{R(x)}\frac{\partial^2}{\partial x^2} + \frac{(B_{12}+B_{22}+2B_{66})\sin\alpha}{R^2(x)}\frac{\partial^2}{\partial\theta^2} + B_{22}\frac{\sin^2\alpha}{R^2(x)}\frac{\partial}{\partial x},$$

$$L_{21} = \frac{(A_{12}+A_{66})}{R(x)}\frac{\partial^2}{\partial x\partial\theta} + \frac{(A_{22}+A_{66})\sin\alpha}{R^2(x)}\frac{\partial}{\partial\theta} + \frac{(B_{12}+B_{66})\cos\alpha}{R^2(x)}\frac{\partial^2}{\partial x\partial\theta} + \frac{(B_{22}-B_{66})\sin\alpha\cos\alpha}{R^3(x)}\frac{\partial}{\partial\theta},$$

$$L_{22} = A_{66}\left[\frac{\partial^2}{\partial x^2} + \frac{\sin\alpha}{R(x)}\frac{\partial}{\partial x} - \frac{\sin^2\alpha}{R^2(x)}\right] + \left[\frac{A_{22}}{R^2(x)} + 2B_{22}\frac{\cos\alpha}{R^3(x)} + \frac{D_{22}\cos^2\alpha}{R^4(x)}\right]\frac{\partial^2}{\partial\theta^2} + 2\frac{D_{66}\cos^2\alpha}{R^2(x)}\left[\frac{\partial^2}{\partial x^2} - \frac{2\sin\alpha}{R(x)}\frac{\partial}{\partial x} + \frac{2\sin^2\alpha}{R^2(x)}\right] + \frac{B_{66}\cos\alpha}{R(x)}\left[3\frac{\partial^2}{\partial x^2} - \frac{\sin\alpha}{R(x)}\frac{\partial}{\partial x} + \frac{\sin^2\alpha}{R^2(x)}\right],$$

$$L_{23} = \left(\frac{A_{22}\cos\alpha}{R^2(x)} + \frac{B_{22}\cos\alpha}{R^3(x)} - \frac{4D_{66}\cos\alpha\sin^2\alpha}{R^4(x)}\right)\frac{\partial}{\partial\theta} - \left(\frac{B_{22}}{R^3(x)} + \frac{D_{22}\cos\alpha}{R^4(x)}\right)\frac{\partial^3}{\partial\theta^3}$$
$$- \left(\frac{B_{22}}{R^2(x)} + \frac{(D_{22}-4D_{66})\sin\alpha\cos\alpha}{R^3(x)}\right)\frac{\partial^2}{\partial x\partial\theta}$$
$$- \left(\frac{(B_{12}+2B_{66})}{R(x)} + \frac{(D_{12}+2D_{66})\cos\alpha}{R^2(x)}\right)\frac{\partial^3}{\partial x^2\partial\theta},$$

$$L_{31} = -A_{12}\frac{\cos\alpha}{R(x)}\frac{\partial}{\partial x} - A_{22}\frac{\sin\alpha\cos\alpha}{R^2(x)} + B_{11}\frac{\partial^3}{\partial x^3} + \frac{(B_{12}+2B_{66})}{R^2(x)}\frac{\partial^3}{\partial x\partial\theta^2}$$
$$- \frac{2B_{11}\sin\alpha}{R(x)}\frac{\partial^2}{\partial x^2} + \frac{B_{22}\sin^2\alpha}{R^2(x)}\frac{\partial}{\partial x} + \frac{(B_{22}-2B_{66})\sin\alpha}{R^3(x)}\frac{\partial^2}{\partial\theta^2} + \frac{B_{22}\sin^3\alpha}{R^3(x)}$$

$$L_{32} = -\left[A_{22}\frac{\cos\alpha}{R^2(x)} - \frac{[B_{22}\cos^2\alpha - (B_{22}+2B_{66})\sin^2\alpha}{R^3(x)}\right]\frac{\partial}{\partial\theta}$$
$$\times\left[-\frac{(2D_{12}+2D_{22}+8D_{66})\cos\alpha\sin^2\alpha}{R^4(x)}\right]\frac{\partial}{\partial\theta} + \left(\frac{B_{22}}{R^3(x)} + \frac{D_{22}\cos\alpha}{R^4(x)}\right)\frac{\partial^3}{\partial\theta^3}$$
$$+\left[\frac{(B_{12}+2B_{66})}{R(x)} + \frac{(D_{12}+4D_{66})\cos\alpha}{R^2(x)}\right]\frac{\partial^3}{\partial x^2\partial\theta}$$
$$+\left[\frac{(B_{22}+2B_{66})\sin\alpha}{R^2(x)} + \frac{(D_{22}+2D_{12+}8D_{66})\sin\alpha\cos\alpha}{R^3(x)}\right]\frac{\partial^2}{\partial x\partial\theta},$$

$$L_{33} = -A_{22}\frac{\cos^2\alpha}{R^2(x)} - \frac{2B_{12}\cos\alpha}{R(x)}\frac{\partial^2}{\partial x^2} + \frac{2B_{22}\cos\alpha}{R^3(x)}\frac{\partial^2}{\partial\theta^2} + \frac{B_{22}\cos\alpha\sin^2\alpha}{R^3(x)}$$
$$\times D_{11}\frac{\partial^4}{\partial x^4} - \frac{2(D_{12}+2D_{66})}{R^2(x)}\frac{\partial^4}{\partial x^2\partial\theta^2} - \frac{D_{22}}{R^4(x)}\frac{\partial^4}{\partial\theta^4}$$
$$- \frac{2D_{11}\sin\alpha}{R(x)}\frac{\partial^3}{\partial x^3} + \frac{2(D_{12}+4D_{66})\sin\alpha}{R^3(x)}\frac{\partial^3}{\partial x\partial\theta^2} + \frac{D_{22}\sin^2\alpha}{R^2(x)}\frac{\partial^2}{\partial x^2}$$
$$- \frac{2(D_{12}+D_{22}+4D_{66})\sin^2\alpha}{R^4(x)}\frac{\partial^2}{\partial\theta^2} - \frac{D_{22}\sin^3\alpha}{R^3(x)}\frac{\partial}{\partial x}. \tag{A.1}$$

Appendix B

The coefficients in Eq. (43) are given by:

$$G_{111} = -A_{22}\frac{\sin^2\alpha}{R^2(x)} - A_{66}\frac{n^2}{R^2(x)},$$

$$G_{112} = A_{11}\frac{\sin\alpha}{R(x)},$$

$$G_{113} = A_{11},$$

$$G_{121} = -\frac{(A_{22}+A_{66})}{R^2(x)}n\sin\alpha - \frac{(B_{12}+B_{22}+2B_{66})}{R^3(x)}n\sin\alpha\cos\alpha,$$

$$G_{122} = \frac{(A_{12}+A_{66})}{R(x)}n + \frac{(B_{12}+2B_{66})}{R^2(x)}n\cos\alpha,$$

$$G_{131} = -A_{22}\frac{\sin\alpha\cos\alpha}{R^2(x)} - \frac{(B_{12}+B_{22}+2B_{66})n^2\sin\alpha}{R^3(x)},$$

$$G_{132} = A_{12}\frac{\cos\alpha}{R(x)} + B_{22}\frac{\sin^2\alpha}{R^2(x)} + \frac{(B_{12}+2B_{66})n^2}{R^2(x)},$$

$$G_{133} = -B_{11}\frac{\sin\alpha}{R(x)},$$

$$G_{134} = -B_{11},$$

$$G_{211} = -\frac{(A_{22}+A_{66})}{R^2(x)}n\sin\alpha - \frac{(B_{22}-B_{66})}{R^3(x)}n\sin\alpha\cos\alpha,$$

$$G_{212} = -\frac{n\cos\alpha}{R^2(x)}(B_{12}+B_{66}) - \frac{n}{R(x)}(A_{12}+A_{66}),$$

$$G_{221} = -\frac{(A_{22}n^2+A_{66}\sin^2\alpha)}{R^2(x)} - \frac{(2B_{22}n^2-B_{66}\sin^2\alpha)}{R^3(x)}\cos\alpha - \frac{(D_{22}n^2-4D_{66}\sin^2\alpha)\cos^2\alpha}{R^4(x)},$$

$$G_{222} = \frac{A_{66}\sin\alpha}{R(x)} - \frac{B_{66}\sin\alpha\cos\alpha}{R^2(x)} - \frac{4D_{66}\sin\alpha\cos^2\alpha}{R^3(x)},$$

$$G_{223} = A_{66} + \frac{3B_{66}\cos\alpha}{R(x)} + \frac{2D_{66}\cos^2\alpha}{R^2(x)},$$

$$G_{231} = -\frac{A_{22}n\cos\alpha}{R^2(x)} - \frac{B_{22}n(\cos^2\alpha+n^2)}{R^3(x)} - \frac{(D_{22}n^2-4D_{66}\sin^2\alpha)n\cos\alpha}{R^4(x)},$$

$$G_{232} = \frac{B_{22}n\sin\alpha}{R^2(x)} + \frac{(D_{22}-4D_{66})n\cos\alpha\sin\alpha}{R^3(x)},$$

$$G_{311} = -\frac{A_{22}\cos\alpha\sin\alpha}{R^2(x)} + \frac{(-B_{22}n^2+2B_{66}n^2+B_{22}\sin^2\alpha)\sin\alpha}{R^3(x)},$$

$$G_{312} = -\frac{A_{12}\cos\alpha}{R(x)} - \frac{(-B_{12}n^2+2B_{66}n^2+B_{22}\sin^2\alpha)}{R^2(x)},$$

$$G_{313} = \frac{2B_{11}\sin\alpha}{R(x)},$$

$$G_{314} = B_{11},$$

$$G_{321} = -\frac{(A_{22}n\cos\alpha)}{R^2(x)} + \frac{(-D_{22}n^2+2D_{12}\sin^2\alpha+2D_{22}\sin^2\alpha+8D_{66}\sin^2\alpha)n\cos\alpha}{R^4(x)} + \frac{(-B_{22}n^2-B_{22}\cos^2\alpha+B_{22}\sin^2\alpha+2B_{66}\sin^2\alpha)n}{R^3(x)},$$

$$G_{322} = \frac{(-D_{22}+2D_{12}+8D_{66})n\cos\alpha\sin\alpha}{R^3(x)} - \frac{(-B_{22}+2B_{66})n\sin\alpha}{R^2(x)},$$

$$G_{323} = \frac{(B_{12}+2B_{66})n}{R(x)} + \frac{(D_{12}+4D_{66})n\cos\alpha}{R^2(x)},$$

$$G_{331} = -\frac{A_{22}\cos^2\alpha}{R^2(x)} + \frac{(-2n^2+\sin^2\alpha)B_{22}\cos\alpha}{R^3(x)} + \frac{(-D_{22}n^2+2D_{12}\sin^2\alpha+2D_{22}\sin^2\alpha+8D_{66}\sin^2\alpha)n^2}{R^4(x)},$$

$$G_{332} = -\frac{(D_{22}\sin^2\alpha + 2D_{12}n^2 + 8D_{66}n^2)\sin\alpha}{R^3(x)},$$

$$G_{333} = \frac{2B_{12}\cos\alpha}{R(x)} + \frac{2D_{12}n^2 + 4D_{66}n^2 + D_{22}\sin^2\alpha}{R^2(x)},$$

$$G_{334} = -\frac{2D_{11}}{R(x)}\sin\alpha, \quad G_{335} = -D_{11}. \tag{B.1}$$

References

[1] M. Bacon, C.W. Bert, Unsymmetric free vibrations of orthotropic sandwich shells of revolution, AIAA J. 5 (1967) 413–417.
[2] C.W. Bert, P.H. Francis, Composite material mechanics: structural mechanics, AIAA J. 12 (1974) 1173–1186.
[3] C.H. Chang, Vibration of conical shells, Shock Vibration Digest 13 (1) (1981) 9–17.
[4] Ö. Civalek, Finite Element Analyses of Plates and Shells, Elaziğ, Firat University, 1998 (in Turkish).
[5] Ö.Civalek, Geometrically non-linear static and dynamic analysis of plates and shells resting on elastic foundation by the method of polynomial differential quadrature (PDQ), Ph.D. Thesis, Firat University, Elazig, 2004 (in Turkish).
[6] Ö. Civalek, An efficient method for free vibration analysis of rotating truncated conical shells, Internat. J. Pressure Vessels Piping 83 (2006) 1–12.
[7] L. Hua, Frequency characteristics of a rotating truncated circular layered conical shell, Composite Structures 50 (2000) 59–68.
[8] L. Hua, Frequency analysis of rotating truncated circular orthotropic conical shells with different boundary conditions, Composites Sci. Technol. 60 (2000) 2945–2955.
[9] L. Hua, K.Y. Lam, The generalized differential quadrature method for frequency analysis of a rotating conical shell with initial pressure, Internat. J. Numer. Methods Eng. 48 (2000) 1703–1722.
[10] T. Irie, G. Yamada, Y. Kaneko, Free vibration of a conical shell with variable thickness, J. Sound Vibration 82 (1982) 83–94.
[11] T. Irie, G. Yamada, K. Tanaka, Natural frequencies of truncated conical shells, J. Sound Vibration 92 (3) (1984) 447–453.
[12] R.K. Kapania, A review on the analysis of laminated shells, Trans. ASME J. Pressure Vessel Technol. 111 (1989) 88–96.
[13] K.Y. Lam, Li Hua, Vibration analysis of rotating truncated circular conical shell, Internat. J. Solids and Structures 34 (17) (1997) 2183–2197.
[14] K.Y. Lam, C.T. Loy, Analysis of rotating laminated cylindrical shells by different shell theories, J. Sound Vibration 186 (1) (1995) 23–35.
[15] A.W. Leissa, Vibration of shells, NASA, SP-288, 1973.
[16] K.M. Liew, Z.C. Feng, Vibration characteristics of conical shell panels with three-dimensional flexibility, J. Appl. Mech. 67 (2) (2000) 314–320.
[17] K.M. Liew, C.W. Lim, Vibratory characteristics of cantilevered rectangular shallow shells of variable thickness, AIAA J. 32 (2) (1994) 387–396.
[18] K.M. Liew, C.W. Lim, Vibration of perforated doubly-curved shallow shells with rounded corners, Internat. J. Solids and Structures 31 (11) (1994) 1519–1536.
[19] K.M. Liew, M.K. Lim, C.W. Lim, D.B. Li, Y.R. Zhang, Effects of initial twist and thickness variation on the vibration behaviour of shallow conical shells, J. Sound Vibration 180 (2) (1995) 272–296.
[20] K.M. Liew, T.Y. Ng, X. Zhao, Vibration of axially loaded rotating cross-ply laminated cylindrical shells via Ritz method, J. Eng. Mech. ASCE 128 (9) (2002) 1001–1007.
[21] K.M. Liew, T.Y. Ng, X. Zhao, Free vibration analysis of conical shells via the element-free kp-Ritz method, J. Sound Vibration 281 (3–5) (2005) 627–645.
[22] C.W. Lim, S. Kitipornchai, Effects of subtended and vertex angles of the free vibration of open conical shell panels: a conical co-ordinate approach, J. Sound Vibration 219 (5) (1999) 813–835.
[23] C.W. Lim, Z.R. Li, G.W. Wei, DSC-Ritz method for high-mode frequency analysis of thick shallow shells, Internat. J. Numer. Methods Eng. 62 (2005) 205–232.
[24] C.W. Lim, Z.R. Li, Y. Xiang, G.W. Wei, C.M. Wang, On the missing modes when using the exact frequency relationship between Kirchhoff and Mindlin plates, Adv. Vibration Eng. 4 (2005) 221–248.
[25] C.W. Lim, K.M. Liew, A pb-2 Ritz formulation for flexural vibration of shallow cylindrical shells of rectangular planform, J. Sound Vibration 173 (3) (1994) 343–375.
[26] C.W. Lim, K.M. Liew, Vibratory behaviour of shallow conical shells by a global Ritz formulation, Eng. Structures 17 (1) (1995) 63–70.
[27] C.W. Lim, K.M. Liew, Vibration of shallow conical shells with shear flexibility: a first-order theory, Internat. J. Solids and Structures 33 (4) (1996) 451–468.
[28] C.W. Lim, K.M. Liew, S. Kitipornchai, Free vibration of pretwisted, cantilevered composite shallow conical, AIAA J. 35 (1995) 327–333.
[29] C.W. Lim, K.M. Liew, S. Kitipornchai, Vibration of cantilevered laminated composite shallow conical shells, Internat. J. Solids and Structures 35 (15) (1998) 1695–1707.
[30] A.E.H. Love, On the small free vibrations and deformations of thin elastic shells, Philos. Trans. Roy. Soc. London 179A (1988) 491–546.
[31] C.H.W. Ng, Y.B. Zhao, G.W. Wei, Comparison of discrete singular convolution and generalized differential quadrature for the vibration analysis of rectangular plates, Comput. Methods Appl. Mech. Eng. 193 (2004) 2483–2506.
[32] J.N. Reddy, Mechanics of composite plates and shells, Theory and Analysis, CRC Press, Boca Raton, FL, 1996.
[33] C. Shu, Free vibration analysis of composite laminated conical shells by generalized differential quadrature, J. Sound Vibration 194 (4) (1996) 587–604.

[34] C. Shu, An efficient approach for free vibration analysis of conical shells, Internat. J. Mech. Sci. 38 (8/9) (1996) 935–949.
[35] C. Shu, H. Du, Free vibration analysis of laminated composite cylindrical shells by DQM, Composites Part B 28 (1997) 267–274.
[36] C.C. Siu, C.W. Bert, Free vibrational analysis of sandwich conical shells with free edges, J. Acoust. Soc. Amer. 47 (1970) 943–945.
[37] K.R. Sivadas, N. Ganesan, Vibration analysis of thick composite clamped conical shells with variable thickness, J. Sound Vibration 152 (1992) 27–37.
[38] W. Soedel, Vibrations of Shells and Plates, second ed., Revised and Expanded, Marcel Dekker Inc., New York, 1996.
[39] L. Tong, Free vibration of orthotropic conical shells, Internat. J. Eng. Sci. 31 (5) (1993) 719–733.
[40] L. Tong, Free vibration of composite laminated conical shells, Internat. J. Mech. Sci. 35 (1) (1993) 47–61.
[41] L. Tong, Free vibration of laminated conical shells including transverse shear deformation, Internat. J. Solids Structure 31 (1994) 443–456.
[42] D.C. Wan, Y.C. Zhou, G.W. Wei, Numerical solution of unsteady incompressible flows by the discrete singular convolution, Internat. J. Numer. Methods Fluid 38 (2002) 789–810.
[43] G.W. Wei, Discrete singular convolution for the solution of the Fokker–Planck equations, J. Chem. Phys. 110 (1999) 8930–8942.
[44] G.W. Wei, Discrete singular convolution for the sine-Gordon equation, Phys. D 137 (2000) 247–259.
[45] G.W. Wei, Wavelets generated by using discrete singular convolution kernels, J. Phys. A 33 (2000) 8577–8596.
[46] G.W. Wei, Solving quantum eigenvalue problems by discrete singular convolution, J. Phys. B 33 (2000) 343–352.
[47] G.W. Wei, A new algorithm for solving some mechanical problems, Comput. Methods Appl. Mech. Eng. 190 (2001) 2017–2030.
[48] G.W. Wei, Vibration analysis by discrete singular convolution, J. Sound Vibration 244 (2001) 535–553.
[49] G.W. Wei, Discrete singular convolution for beam analysis, Eng. Structures 23 (2001) 1045–1053.
[50] G.W. Wei, G. Yun, Conjugate filter approach for solving Burgers' equation, J. Comput. Appl. Math. 149 (2002) 439–456.
[51] G.W. Wei, Y.B. Zhao, Y. Xiang, The determination of natural frequencies of rectangular plates with mixed boundary conditions by discrete singular convolution, Internat. J. Mech. Sci. 43 (2001) 1731–1746.
[52] G.W. Wei, Y.B. Zhao, Y. Xiang, Discrete singular convolution and its application to the analysis of plates with internal supports. Part 1: theory and algorithm, Internat. J. Numer. Methods Eng. 55 (2002) 913–946.
[53] G.W. Wei, Y.B. Zhao, Y. Xiang, A novel approach for the analysis of high-frequency vibrations, J. Sound Vibration 257 (2) (2002) 207–246.
[54] C.-P. Wu, .Wu C-H, Asymptotic differential quadrature solutions for the free vibration of laminated conical shells, Computat. Mech. 25 (2000) 346–357.
[55] C.C. Yang, On vibrations of orthotropic conical shells, J. Sound Vibration 34 (1974) 552–555.
[56] H. Yunshan, G.W. Wei, Y. Xiang, DSC-Ritz method for the free vibration analysis of Mindlin plates, Internat. J. Numer. Methods Eng. 62 (2005) 262–288.
[57] S. Zhao, G.W. Wei, Y. Xiang, DSC analysis of free-edged beams by an iteratively matched boundary method, J. Sound Vibration 284 (2005) 487–493.
[58] Y.B. Zhao, G.W. Wei, DSC analysis of rectangular plates with non-uniform boundary conditions, J. Sound Vibration 255 (2) (2002) 203–228.
[59] Y.B. Zhao, G.W. Wei, Y. Xiang, Discrete singular convolution for the prediction of high frequency vibration of plates, Internat. J. Solids and Structures 39 (2002) 65–88.
[60] Y.B. Zhao, G.W. Wei, Y. Xiang, Plate vibration under irregular internal supports, Internat. J. Solids and Structures 39 (2006) 1361–1383.